

Local Field Potential in Cortical Area MT: Stimulus Tuning and Behavioral Correlations

Jing Liu and William T. Newsome

Howard Hughes Medical Institute and Department of Neurobiology, Stanford University School of Medicine, Stanford, California 94305-5125

Low-frequency electrical signals like those that compose the local field potential (LFP) can be detected at substantial distances from their point of origin within the brain. It is thus unclear how useful the LFP might be for assessing local function, for example, on the spatial scale of cortical columns. We addressed this problem by comparing speed and direction tuning of LFPs obtained from middle temporal area MT with the tuning of multiunit (MU) activity recorded simultaneously. We found that the LFP can be well tuned for speed and direction and is highly correlated with that of MU activity, particularly for frequencies at and above the gamma band. LFP tuning is substantially poorer for lower frequencies, although tuning for direction extends to lower frequencies than does tuning for speed. Our data suggest that LFP signals at and above the gamma band reflect neural processing on the spatial scale of cortical columns, within a few hundred micrometers of the electrode tip. Consistent with this notion, we also found that frequencies at and above the gamma band measured during a speed discrimination task exhibit an effect known as “choice probability,” which reveals a particularly close relationship between neural activity and behavioral choices. In the LFP, this signature of the perceptual choice comprises a shift in relative power from low-frequency bands (α and β) to the gamma band. It remains to be determined how LFP choice probability, which is a temporal signature, is related to conventional choice probability effects observed in spike rates.

Key words: LFP; spectral component; MT; visual motion; extrastriate; choice probability

Introduction

The local field potential (LFP) is composed of low-frequency extracellular voltage fluctuations that are thought to reflect synaptic potentials (Mitzdorf, 1987) and other slow electrical signals such as spike afterpotentials and voltage-dependent membrane oscillations (for review, see Logothetis, 2003). Neurophysiologists have used the LFP with increasing frequency in recent years to link neural activity to perception and cognition, including sensory stimuli coding, perceptual binding, attention, and working memory (Kruse and Eckhorn, 1996; Fries et al., 2001; Pesaran et al., 2002; Siegel and Konig, 2003; Gail et al., 2004; Henrie and Shapley, 2005; Rickert et al., 2005; Scherberger et al., 2005; Taylor et al., 2005; Womelsdorf et al., 2006). The nature of the LFP, however, remains ambiguous in important ways, including its spatial resolution, which has always been poorly defined. It is well known that low-frequency electrical signals can be recorded at substantial distances from their point of origin within a filtering medium such as the human body. The field of electroencephalography, for example, is based on this principle (Lopes da Silva, 2004). Thus, the question of spatial scale is critical for assessing

how the LFP can contribute to the study of cortical computation and its relationship to behavior.

The central goal of our study was to assess the utility of the LFP signal for evaluating “local” cortical processing on the spatial scale of cortical columns. We therefore compared LFP activity in narrow spectral sub-bands with simultaneously measured multiunit (MU) signals, which are known to reflect local columnar architecture (DeAngelis and Newsome, 1999; Liu and Newsome, 2003). Previous studies have found that gamma-band activity, in contrast to activity at lower frequencies, is tuned for specific features of a visual stimulus, suggesting that gamma-band activity originates from highly local neighborhoods within the cortex (Gray and Singer, 1989; Fries and Eckhorn, 2000; Fries et al., 2000; Fries et al., 2002; Siegel and Konig, 2003; Kayser and Konig, 2004; Henrie and Shapley, 2005). Previous studies, however, did not compare LFP tuning with that of relatively well understood signals such as single-unit (SU) and MU activity, and it is therefore difficult to infer how the LFP is related to cortical architecture.

We approached this problem by comparing the speed and direction tuning of LFP and MU signals recorded simultaneously from the middle temporal visual area (MT). An advantage of this approach is the well documented organization, at different spatial scales, of speed- and direction-tuned neurons in MT. Speed-tuned neurons are organized in highly local clusters of $<500 \mu\text{m}$ in diameter, whereas direction-tuned neurons are organized in stereotypical cortical columns such that neurons separated by as much as 2 mm (perpendicular to the cortical surface) can share a common preferred direction (Albright et al., 1984; DeAngelis and Newsome, 1999; Liu and Newsome, 2003). This difference in

Received Nov. 28, 2005; revised April 20, 2006; accepted May 30, 2006.

This work was supported by National Eye Institute Grant EY05603. W.T.N. is an Investigator of the Howard Hughes Medical Institute. We thank M. Philiastides for designing the notch filter. We also thank A. Batista, K. Britten, M. Churchland, P. Fries, P. Konig, N. Logothetis, J. Reppas, G. Santhanam, M. Shadlen, K. Shenoy, and the anonymous reviewers for helpful discussions on this manuscript.

Correspondence should be addressed to Dr. Jing Liu, Department of Neurobiology, Stanford University School of Medicine, Fairchild Building D209, Stanford, CA 94305. E-mail: jingliu@stanford.edu.

DOI:10.1523/JNEUROSCI.5052-05.2006

Copyright © 2006 Society for Neuroscience 0270-6474/06/267779-12\$15.00/0

spatial organization, in combination with quantitative measurements of direction and speed tuning, permits inferences concerning the spatial origin of different spectral sub-bands of the LFP.

In a second experiment, we measured the LFP from MT while monkeys performed a two-alternative, forced-choice speed discrimination task (Liu and Newsome, 2005). We observed a trial-to-trial correlation in the temporal organization of the LFP and perceptual judgments of speed. This effect appears to be a temporal correlate of the well known “choice probability” (CP), which reflects a trial-to-trial correlation between spike counts and perceptual judgments of direction and speed (Krug, 2004).

Materials and Methods

Monkey maintenance and surgery. We conducted extracellular recordings in three hemispheres of two macaque monkeys (*Macaca mulatta*), one male and one female. Before the experiments, the monkeys were surgically implanted with a head-holding device and recording cylinder (Crist Instruments, Hagerstown, MD) and a scleral search coil for monitoring eye position. All implanted devices were magnetic resonance imaging compatible. Surgical, animal care, and experimental procedures conformed to guidelines established by the National Institutes of Health and were approved in advance by the Stanford University Institutional Animal Care and Use Committee.

Visual stimuli. During each experimental session, the monkey was seated in a primate chair with its head fixed. The monkey viewed visual stimuli on a cathode ray tube monitor at a distance of 57 cm. Visual stimuli were drawn with a VSG graphics board (Cambridge Research Systems, Kent, UK); the frame rate of the monitor was 160 Hz.

In both the fixation and speed discrimination tasks, the visual stimuli were white random dots in fully coherent motion on a black background (Britten et al., 1992). The size of each dot was $0.2 \times 0.2^\circ$, and the dot density was 0.6 dots per square degree. To maintain a constant dot density, each dot that left the aperture reentered from the other side at a random location.

Behavioral tasks. We measured direction and speed tuning curves while the monkeys performed a fixation task (Liu and Newsome, 2003). Random dot stimuli appeared for 1 s inside a circular aperture that was centered on and filled the receptive field (RF) of the MU (Fig. 1A). To acquire a reward, the monkeys simply maintained eye position within an electronic window ($2 \times 2^\circ$) surrounding a central fixation cross ($0.3 \times 0.3^\circ$).

We used a spatial two-alternative forced-choice (2-AFC) speed discrimination task (Fig. 1B) to investigate the relationship between electrophysiological measures and perceptual judgments (Liu and Newsome, 2005). While maintaining fixation on a central fixation cross, the monkey viewed two groups of moving random dots (for 1 s) inside two apertures, positioned symmetrically around the fixation cross in opposite hemifields. During recording, one aperture was always positioned in the MU RF. Motion direction was the same in the two apertures, but the speed differed slightly between the two in each trial. At 200 ms after the visual stimulus disappeared, a saccade target appeared in the center of each aperture, and the fixation cross disappeared. The monkeys indicated which dot group moved faster by making a saccadic eye movement to the corresponding target. Speed differences between the two apertures covered a range spanning psychophysical threshold and are expressed in all figures as percentage speed difference (the difference between the two speeds divided by the faster speed). Large speed differences yielded near-perfect discrimination behavior, whereas small speed differences yielded near-chance behavior. The range of speeds used was adjusted for each experiment so as to match the steepest part of the speed tuning curve measured at the recording site (Liu and Newsome, 2005).

Recording cylinder locations and data collection. We used tungsten microelectrodes with impedances of ~ 0.5 – $1 \text{ M}\Omega$ (Frederick Haer Company, Bowdoinham, ME), introduced to the cortex through a transdural guide tube positioned within a plastic grid inside the recording cylinder. To access MT, we placed the recording cylinders either posteriorly so that microelectrodes crossed primary visual cortex V1 and the lunate sulcus before reaching MT or anteriorly so that microelectrodes crossed the

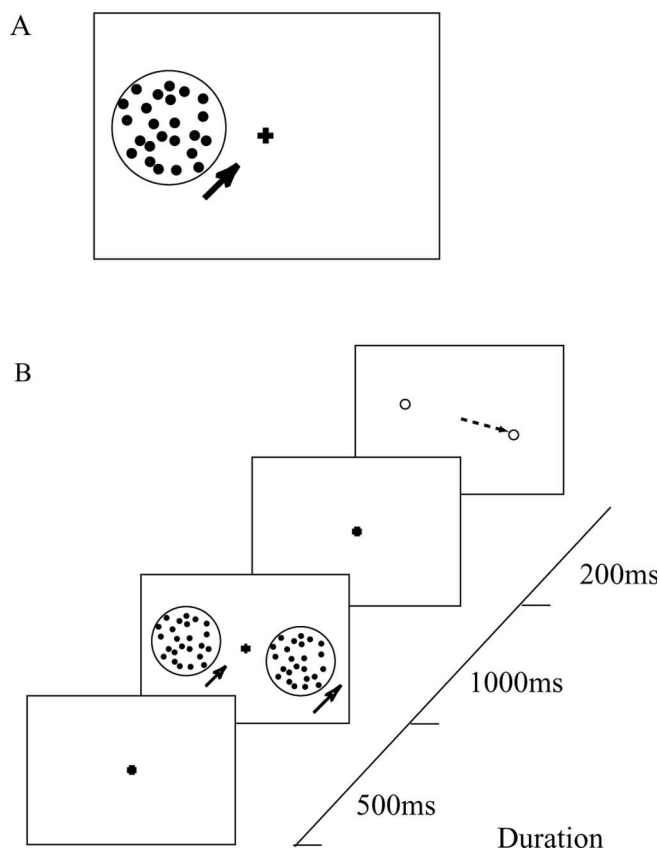


Figure 1. Schematic illustration of the behavioral tasks. **A**, Fixation task. The monkey was required to maintain fixation on the central cross while tuning curves were measured using visual stimuli positioned in the MU RF. **B**, Spatial 2-AFC speed discrimination task. The monkey fixated the central cross for 500 ms at the beginning of the trial, and the visual stimuli then appeared for 1 s. After the disappearance of the visual stimuli, the two saccade targets appeared inside the visual stimulus apertures. After another 200 ms, the fixation point disappeared, giving the monkey permission to execute the operant saccade.

central sulcus, the intraparietal sulcus, and the anterior bank of the superior temporal sulcus before reaching MT. We identified MT on the basis of its characteristic direction tuning, RF size, topography, and depth below the cortical surface (van Essen et al., 1981).

Electrodes were advanced in the brain using a hydraulic microdrive (Narishige, Tokyo, Japan). The LFP signals were obtained by analog filtering of the raw voltage trace, with a low-cutoff frequency at 3 or 10 Hz and a high-cutoff frequency at 150 Hz (Krohn-Hite, Brockton, MA) (Fig. 2A), and then digitized at 500 or 1 kHz. At 13 of the 252 recording sites, the high-cutoff frequency was 200 Hz (four sites) or 300 Hz (nine sites). All population results presented in this paper remained the same if these 13 sites were excluded from the analysis.

For MU recordings, neural voltage signals were amplified, filtered (500 Hz to 6 kHz), with filter characteristics of 30 dB/octave for low frequency and 12 dB/octave for high frequency (Bak Electronics, Germantown, MD), and displayed on an oscilloscope. We considered a “neural event” to be any deflection of the voltage trace above an arbitrarily determined threshold amplitude within a fixed time window. This threshold was set manually so that the “spontaneous” activity in the absence of a visual stimulus was between 50 and 100 events/s.

At each recording site, we first used an interactive stimulus presentation program to assess qualitatively the location and size of the RF, as well as the preferred direction and speed of the MU. We then measured speed and direction tuning properties quantitatively after centering the random dot stimulus on the RF and adjusting the size of the aperture to match the size of the RF (Liu and Newsome, 2003).

For all experiments and all electrophysiological measures, we considered visual responses to be the average activity recorded during the 1 s

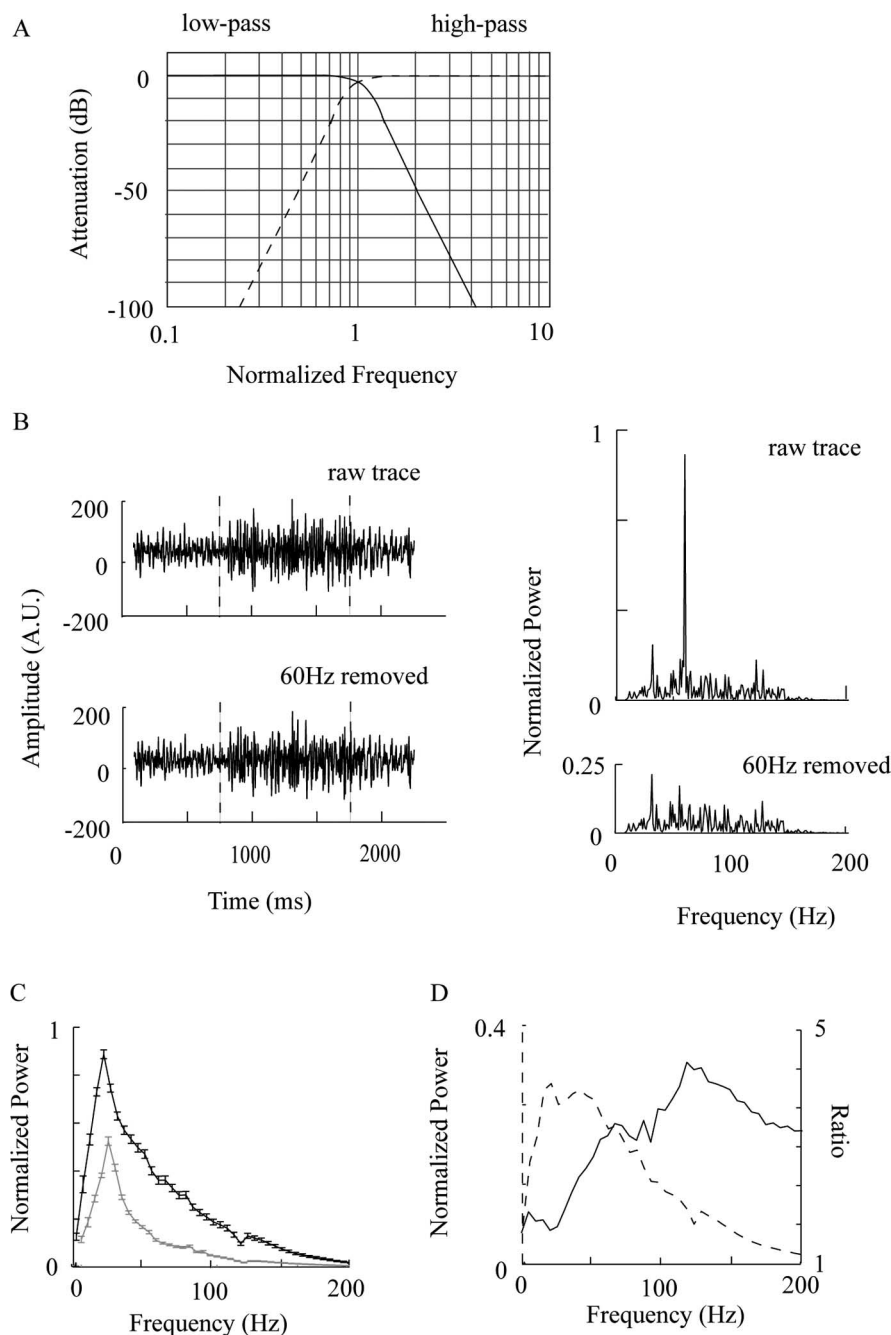


Figure 2. *A*, Filter characteristics (adapted from Krohn-Hite model 3384 user's manual). The attenuation is plotted against frequencies normalized to the high- or low-cutoff frequency. *B*, The LFP signal in one trial during the measurement of a speed tuning curve. The top left panel shows the raw voltage trace; the bottom left panel shows the same trace with 60 Hz noise removed. The two vertical lines indicate stimulus onset and offset. The right panels illustrate the power spectra of the two single traces depicted in the left panels. *C*, Average power for all speed tuning data. Power was computed within 5 Hz bins for each individual trial, averaged over all trials within a block, normalized by the peak power within the block, and then averaged across all sites for which speed tuning curves were collected. We excluded sites that showed strong inhibitory effects (Fig. 8, Table 2), sites that were not tuned for speed, and sites in which the high-cutoff frequency for the LFP exceeded 150 Hz. The black trace represents the power spectrum during visual stimulus presentation. The gray trace represents the power spectrum of the spontaneous activity. Error bars indicate the SEM. Note that the spontaneous activity was also normalized by the peak of the spectrum during visual stimulus presentation, this is why the spontaneous activity is never close to unity. Each data point is the average power within a 5 Hz window. *D*, The dashed line is the modulation of LFP power attributable to the visual stimulus, which is simply the difference between the two traces in *C*. The scale of this trace is indicated on the y-axis at the left margin of the graph. The black line is the ratio of the two traces in *C*, which is the visual response gain as a function of frequency. The y-axis at the right margin of the plot shows the scale for the ratio values.

stimulus presentation interval. Spontaneous activity was calculated as the average activity during the 750 ms interval preceding onset of the visual stimulus.

Signal processing. We removed 60 Hz noise (and its first harmonic) off-line using an adaptive noise cancellation procedure that filters the original signal in the time domain (Widrow et al., 1975). The primary virtue of the adaptive procedure is that it is tuned separately for each LFP trace, adjusting automatically for variation over time in the exact amplitude, frequency, and structure of the 60 Hz noise. Because the adaptive filtering algorithm involves recurrent comparisons of the input and output signals, best results are in fact obtained when two filters are constructed for each trial, with the spontaneous activity portion of the LFP trace filtered separately from the "visually evoked" portion of the trace. We used this procedure for all LFP data presented in this paper, although no major results changed if we filtered the entire LFP trace with a single filter.

The primary user-controlled parameter of the filter adjusts the aggressiveness of the adaptive process, permitting more rapid adaptation, but at the cost of increased "notch" width. The user's challenge is to maximize the temporal performance of the filter but minimize any distorting effects on the real underlying signal. To accomplish this, we monitored filter performance in the frequency domain by computing a Fourier power spectrum for each filtered LFP signal. In an iterative procedure performed for each LFP trace, the computer gradually increased the value of the control parameter until the power in the 58–62 Hz band fell slightly below the average of the power in the 48–52 and 68–72 Hz bands. Across 2300 arbitrarily selected trials, the final filter width averaged 1.0 Hz, with an SD of 0.8 Hz, confirming that the adaptive procedure produced excellent notch filters.

After noise cancellation, we considered the LFP "response" on a single trial to be the root mean square (RMS) value of the filtered voltage trace. LFP tuning curves were computed from the average RMS values of all LFP traces obtained for each stimulus condition. LFP CP (see below) was computed from RMS values obtained on individual trials.

A central analysis presented in this paper is evaluation of LFP tuning curves and CP within frequency bands of the LFP. We used two methods to divide the LFP into narrower bands. In the first, we calculated the LFP power spectrum [discrete Fourier transform with Matlab (MathWorks, Natick, MA) function "fft"] and used the sum of the power within a specific frequency range as the response for computing physiological tuning curves and CP. (Frequency leakage was not a serious problem because of our long LFP trace—750 or 1000ms). In the second method, we applied FIR filtering (filter designed in Matlab using "fdatool") to the LFP in the time domain to isolate signals in each frequency band, and then considered the RMS of the filtered signal to be the response for computing tuning curves and CP. The results obtained using these two methods

Table 1. Summary of numbers of recorded sites

	Direction tuning curve	Speed tuning curve	CP	Area summation curve
Monkey C	128	129	22	43
Monkey Y	48	50	33	46
Total number of sites	176	179	55	89

were similar, and only results from the first method are included in this paper.

Data analysis: physiological properties. We analyzed speed tuning properties using methods established in our previous studies (Liu and Newsome, 2003). For each speed-tuned site (ANOVA, $p < 0.05$), we fitted the tuning curve with a smoothing cubic spline function (Shikin and Plis, 1995). We considered the “preferred” speed to be the speed that corresponded to the peak of the fitted tuning curve. The width of the tuning curve was defined as the full width of the curve at 90% of the best response ($R_{\max} - R_{\text{spont}}$). We considered a site to be bandpass for speed if the response fell below 90% of the peak response on both sides of the fitted tuning curve, high pass if the response to the fastest speed exceeded 90% of $R_{\max} - R_{\text{spont}}$, and low pass if the response to the slowest speed exceeded 90% of $R_{\max} - R_{\text{spont}}$.

For direction-tuned sites (ANOVA, $p < 0.05$), we fitted the direction responses with a von Mises curve (Mardia, 1972) and considered (1) the preferred direction of the site to be the direction corresponding to the peak of the fitted curve, and (2) the tuning width to be the full width of the curve at 50% of the maximum response ($R_{\max} - R_{\text{spont}}$).

Occasionally we encountered sites for which excitatory visual responses could not be detected in the LFP although they were present in simultaneous MU or SU recordings. At these sites, there was no direction or speed tuning (ANOVA, $p > 0.05$), and the largest response was no different from spontaneous activity (t test, $p > 0.05$). These sites were classified as “unresponsive” in the LFP database (see Table 2). At several other sites, LFP visual responses were speed and direction tuned (ANOVA, $p < 0.05$) but were entirely inhibitory despite the presence of excitatory responses in the MU or SU data (see Table 2).

Data analysis: choice probability. CP is a metric that captures trial-to-trial relationships between neural responses and psychophysical choices in a two-alternative, forced-choice discrimination task, assuming repeated identical presentations of a weak stimulus (Britten et al., 1996; Dodd et al., 2001; Cook and Maunsell, 2002; Uka and DeAngelis, 2004; Barberini et al., 2005; Liu and Newsome, 2005; Purushothaman and Bradley, 2005).

In practice, assessment of CP involves subdividing a distribution of neural responses to a particular stimulus into two subdistributions, each corresponding to one class of behavioral choices in the psychophysical task (e.g., fast or slow). If the subdistributions differ statistically, a relationship between neural response and psychophysical choice is inferred. The subdistributions are typically compared by measuring the area under a receiver operator curve (ROC), a construction derived from the theory of signal detection (Green and Swets, 1966). The resulting metric, the CP, assumes a value of 0.5 if there is no relationship between perceptual decisions and neuronal responses. The CP assumes progressively larger deviations from 0.5 (with 0 as lower bound and 1 as upper bound) for increasingly strong correlations between response fluctuations and perceptual decisions. The statistical significance of an individual CP value is assessed with a permutation test; statistical significance at the population level is assessed by a t test that determines whether the mean CP value differs significantly from 0.5. For a detailed description of the CP calculation and statistical testing, see Britten et al. (1996) or Liu and Newsome (2005).

Results

Database

The results in this paper are based on 234 MT recording sites in two monkeys. Table 1 shows the total number of sites studied in

Table 2. Summary of speed and direction tuning

	Tuned (%)	Untuned (%)	Unresponsive (%)	Inhibitory (%)	<i>n</i>
Speed (LFP)	63.1	17.3	14.5	5	179
Speed (MU activity)	97.8	2.2	0	0	179
Direction (LFP)	54.0	22.1	21.6	2.3	176
Direction (MU activity)	96.6	3.4	0	0	176

each monkey as well as the number of sites for which each individual experiment was completed.

The LFP signals

The left panels of Figure 2*B* depict the LFP signal in a typical trial before and after removal of the 60 Hz noise; the vertical dashed lines delineate the visual stimulus interval. The right panels show the power spectra of the same two LFP signals. The filtering process eliminated 60 Hz noise without distorting the visually evoked signal. Figure 2*C* shows the average of the power spectra of individual LFP traces recorded during an entire block of trials. The black trace is the average spectrum during the visual stimulus period, whereas the gray trace represents the spectrum of the spontaneous activity measured 750 ms before onset of the visual stimulus. The power at frequencies < 5 Hz and > 150 Hz was almost negligible, confirming the efficacy of our on-line filters. Within the pass band of the filters, LFP power decreased with increasing frequency, consistent with many previous studies.

Also consistent with previous studies (Frien et al., 2000; Siegel and Konig, 2003; Henrie and Shapley, 2005), we found that visual stimuli evoked a perceptible increase in LFP power. The visual response is evident in the raw trace in Figure 2*B* as well as in the average power spectra in Figure 2*C*. Differencing the two curves in Figure 2*C* shows that visually evoked activity was greatest in absolute terms near 25 Hz, falling off gradually at progressively higher frequencies (Fig. 2*D*, dashed line). The solid curve in Figure 2*D* shows, however, that the ratio of visually evoked to spontaneous LFP power increased gradually as a function of frequency, achieving a maximum well beyond the conventionally defined gamma band (24–80 Hz). Importantly, the solid curve in Figure 2*D* shows that detecting visually evoked signals relative to other sources of LFP variation is considerably more difficult in the alpha (10–12 Hz) and beta (12–24 Hz) bands than at higher frequencies.

Although the visual response is readily visible in the single LFP trace of Figure 2*B*, visual responses were generally weaker in LFP recordings than in MU or SU recordings. As indicated in Table 2, we were unable to detect any LFP response in 14.5% of the speed tuning measurements and 21.6% of the direction tuning measurements. This may be attributable in part to the fact that we mapped receptive fields and optimized the stimulus aperture size and location based on MU responses, not LFP activity.

Speed and direction tuning of LFP and MU activity

Figure 3 shows an example of speed and direction tuning curves for MU and LFP recordings made simultaneously from a single electrode. Occasionally, we also recorded single neuron activity together with MU and LFP. The recorded SU responses at this site are also shown. LFP speed and direction tuning curves were similar to those of MU and SU activity at this site.

We confirmed this similarity at the population level with a quantitative comparison of the tuning of LFP and MU activity recorded simultaneously (Fig. 4). This population comparison only includes sites for which both signals were tuned, and the

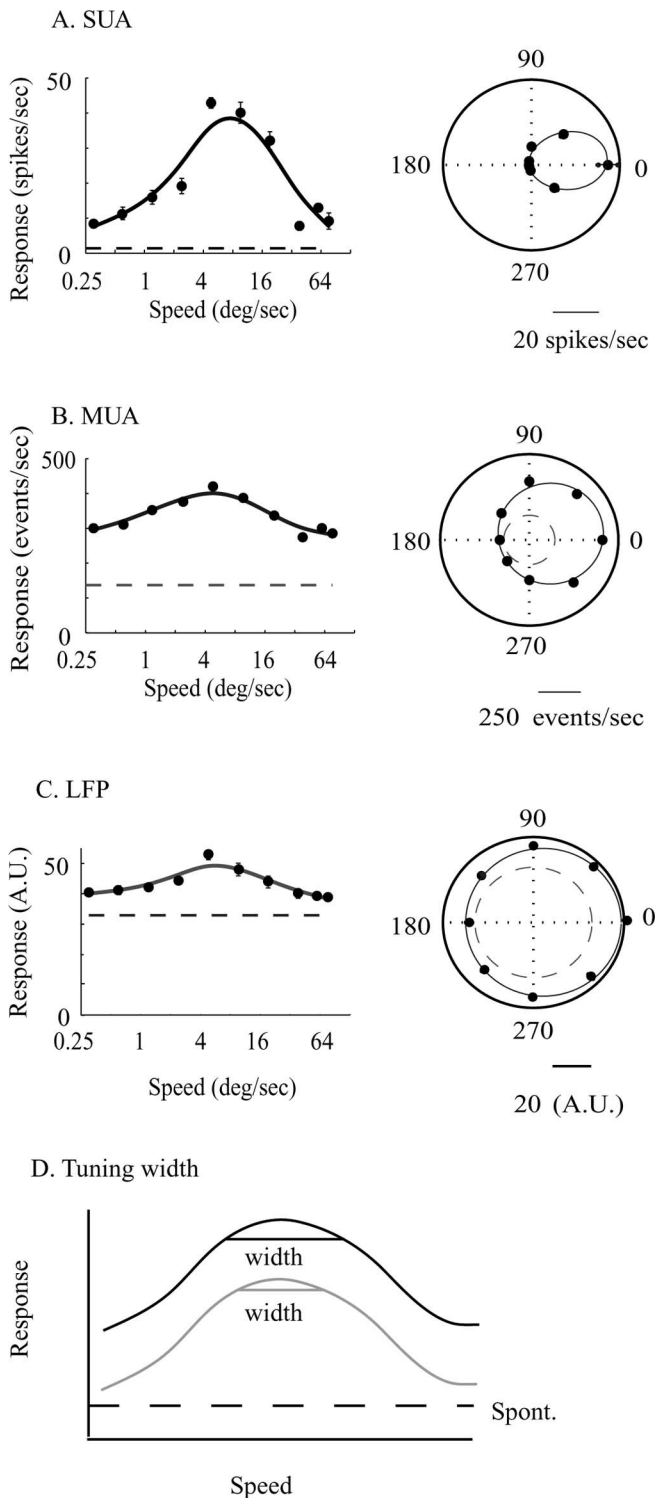


Figure 3. An example of simultaneously recorded SU, MU, and LFP tuning curves. **A**, SU speed (left) and direction (right) tuning curves. **B**, MU tuning curves. **C**, LFP tuning curves. **D**, An illustration of the “iceberg effect.” We defined the width of a tuning curve as the full width of the curve at 90% of the best response, i.e., $0.9 \times (R_{\max} - R_{\text{spont}})$. More pronounced visual modulation (the black curve compared with the gray curve) increases $R_{\max} - R_{\text{spont}}$; consequently, the tuning width also becomes larger. MUA, MU activity; SUA, SU activity; A.U., arbitrary units.

speed tuning curve exhibited a bandpass shape with a well defined optimal speed. [Most investigators also consider a neural activity to be “tuned” for speed if the tuning curve exhibits “high pass” or “low pass” characteristics, but we did not include such

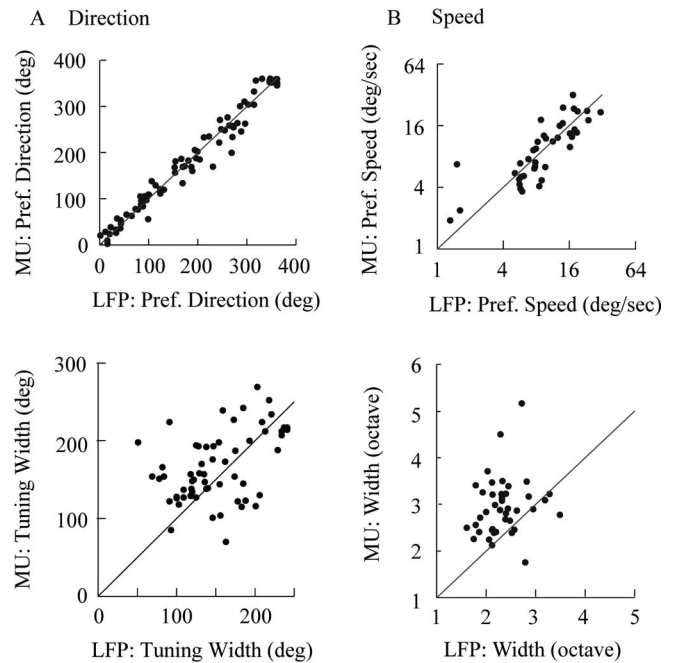


Figure 4. **A**, Comparison of direction tuning properties between MU and LFP recordings. Top, Preferred directions; bottom, tuning widths. **B**, A comparison of speed tuning properties between MU and LFP recordings; only bandpass sites are included in this analysis. Top, Preferred speeds; bottom, tuning widths.

sites in this comparison because it is difficult to identify a specific optimal speed (for details, see Liu and Newsome, 2003)]. Figure 4 thus includes 85 pairs of direction tuning curves and 41 pairs of speed tuning curves (Table 2).

Preferred directions extracted from LFP and MU data were highly correlated ($r = 0.987$; $p < 10^{-46}$) (Fig. 4A, top), as were preferred speeds ($r = 0.809$; $p < 10^{-10}$) (Fig. 4B, top). Moreover, the preferred directions and speeds extracted from MU and LFP data were generally very similar, the data points being clustered about the unity line. Tuning widths were narrower for LFP data than for MU data (Fig. 4A,B, bottom), both for speed (paired t test, $p < 0.01$) and marginally for direction (paired t test, $p < 0.06$). Across the population of experiments, correlation between LFP and MU tuning widths was either weak (for direction, $r = 0.46$; $p < 0.001$) or absent (for speed, $r = 0.175$; $p = 0.27$).

At first glance, the observation of narrower tuning widths for the LFP data appears counterintuitive. This observation, however, almost certainly results from the fact that visual responses were generally weaker in our LFP data than in our MU data (see text above and Table 2). The speed tuning curves in Figure 3, B and C, are very similar for MU and LFP data, but the LFP tuning curve lies closer to the spontaneous activity level than does the MU tuning curve. As Figure 3D illustrates, the same tuning curve will yield progressively narrower tuning widths as the responses sink toward the noise level (“iceberg effect”).

As indicated above, only sites with bandpass speed tuning were included in the analyses of Figure 4. We did check, however, whether the speed tuning category for each site (see Materials and Methods) was consistent for the LFP and MU data. Of 96 pairs of speed-tuned sites, the LFP and the MU data resulted in the same classification for 80 pairs. Sites that were classified differently by the two electrophysiological measures generally lay close to one of the categorization criteria.

Local activity is best represented at frequencies at and above the gamma band

Figure 5 depicts speed tuning curves after dividing the LFP signal into 20-Hz-wide bands, at one recording site. The ordinate shows the summed power of the LFP signal within each band (see Materials and Methods). Speed tuning is absent in the lowest bands, becoming significant only for bands above 40 Hz. Tuning becomes weaker for the highest frequencies, as expected from the low-pass bound of our initial LFP filter (150 Hz).

Figure 6 shows a systematic evaluation of this result at the population level. We assessed speed and direction tuning (Fig. 6*A, B*, respectively) within every possible frequency band between 0 and 200 Hz (10 Hz resolution). In Figure 6, *A* and *B*, the gray level depicts the percentage of sites exhibiting speed or direction tuning by our standard ANOVA criteria (see Materials and Methods). The percentage of tuned sites becomes higher as the frequency band excludes signals below 40 Hz, and the highest percentage of tuned sites occurred above 60 Hz.

The data in Figure 6 suggest that the excellent correlation between LFP and MU preferred speed and direction (Fig. 4) is driven primarily by frequency components at or above the gamma band. Figure 7 provides explicit support for this conclusion. The absolute difference in preferred speed computed from LFP and MU data (averaged across recording sites) is illustrated as a function of frequency (in 20 Hz bands) in Figure 7*A*. The differences are large and highly variable below 60–80 Hz but become small and stable at higher frequencies. A similar trend holds for absolute differences in preferred direction (Fig. 7*C*). We recomputed the correlation between preferred speeds (LFP vs MU) and preferred directions (LFP vs MU) within each 20 Hz frequency band, following the general procedure of Figure 4, *A* and *B*. Figure 7, *B* and *D*, shows the results for preferred speed and preferred direction, respectively. Correlation coefficients became larger and statistically significant (black data points, $p < 0.05$) as the frequency increased. The insets of Figure 7, *B* and *D*, illustrate scatter plots of preferred speeds and preferred directions, respectively, for one low-frequency bin and one high-frequency bin. Correlations are weaker in the low-frequency range for two reasons: 1) fewer sites are tuned, resulting in a smaller database for computing correlation coefficients, and 2) there is substantially more scatter in the data points at low frequencies.

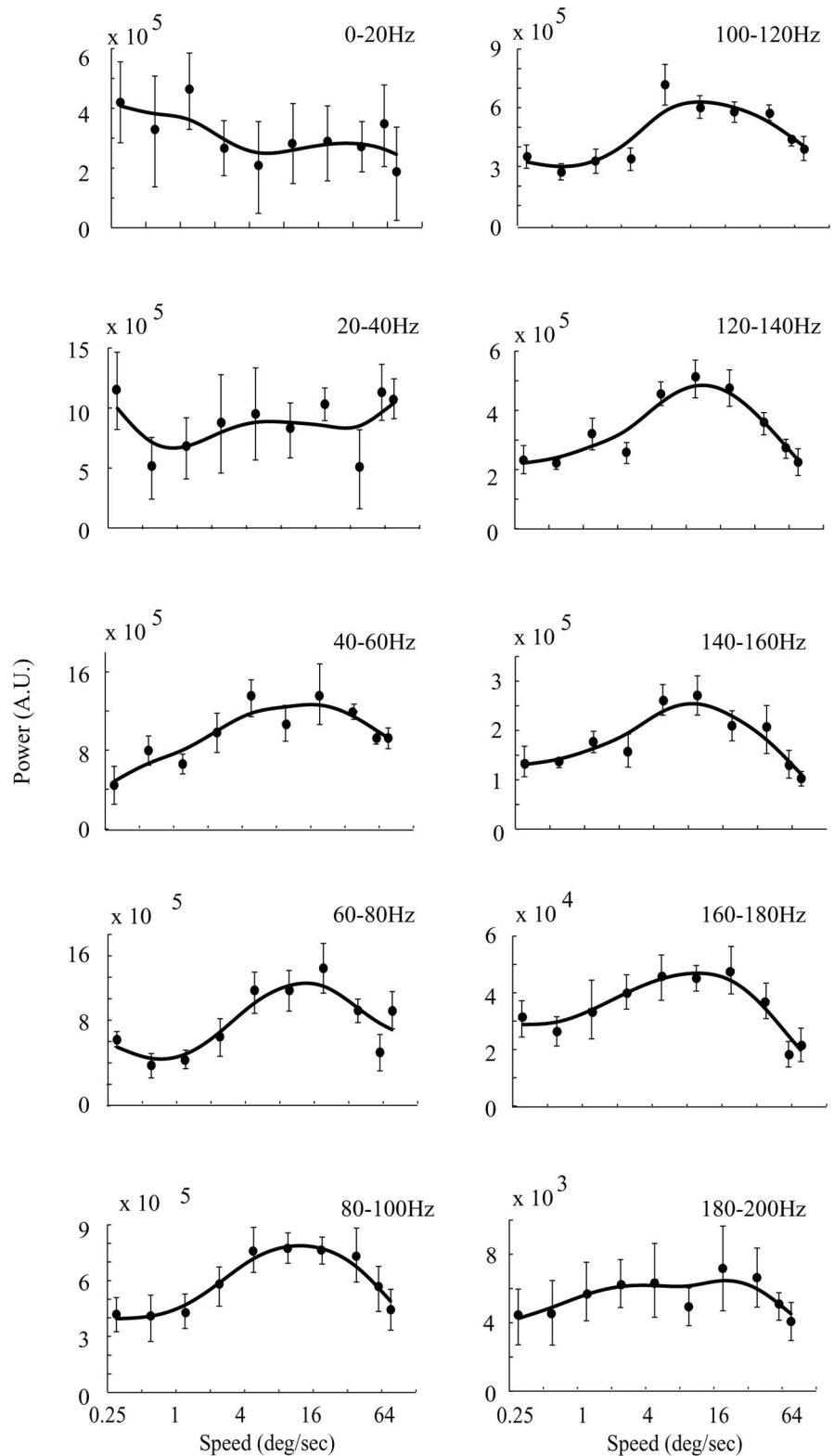


Figure 5. Speed tuning curves of different LFP frequency bands at a speed-tuned site, plotted as the total power within each frequency band as a function of stimulus speed. (Note that the y-axis scale differs among the plots.) We subtracted the spontaneous activity in each trial from the visually evoked activity before plotting the tuning curve. A.U., Arbitrary units.

Figure 7 reveals an important difference in the spectral characteristics of speed and direction tuning of the LFP: tuning stability extends to lower frequencies for direction than for speed. As we inspect the figure from high to low frequencies, the correlation coefficient between LFP and MU preferred speeds begins

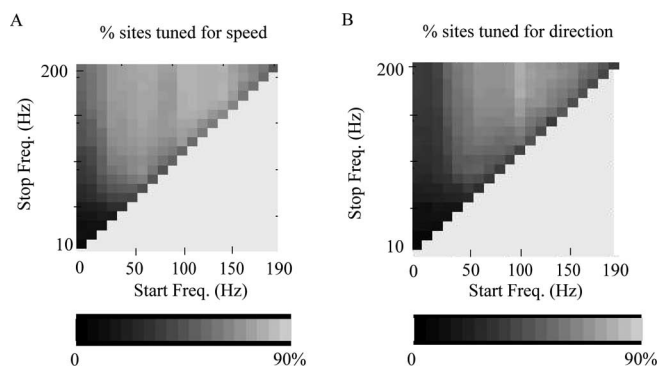


Figure 6. *A*, The percentage of speed-tuned sites among all sites in which LFP signals were recorded, as a function of frequency. The grayscale value (indicated in the color scale below the grid) of each pixel depicts the percentage of speed-tuned sites within a frequency band defined by the low-cutoff value indicated on the x-axis and the high-cutoff value indicated on the y-axis. *B*, The percentage of direction-tuned sites plotted in the same format as in *A*. In both *A* and *B*, each square represents the value of one frequency band, with the low-cutoff frequency indicated on the y-axis and the high-cutoff frequency indicated on the x-axis.

falling for frequencies as high as 100 Hz (Fig. 7*B*), and the absolute difference in preferred speed becomes large and variable near 80 Hz (Fig. 7*A*). For preferred direction, however, the correlation coefficient begins to deteriorate (Fig. 7*D*), and the absolute difference in preferred direction becomes large and variable (Fig. 7*C*), only for frequencies below 40 Hz. This difference in spectral characteristics appears to mirror the known difference in spatial organization of speed-tuned (<500 μm) and direction-tuned (<500 μm tangential but up to 2000 μm perpendicular to the cortical surface) neurons in MT. We will consider the implications of this observation in Discussion.

In a second analysis, we divided the LFP signal into standard frequency bands defined on the basis of electroencephalography measurements: theta (5–8 Hz), alpha (8–12 Hz), beta (16–30 Hz), and gamma (30–100 Hz). The gamma band exhibited strong direction and speed tuning, as described above, but the other bands did not (data not shown).

Differences between LFP and MU data

Several differences between the LFP and the MU data were obvious in our sample. First, as discussed above, LFP recordings failed to yield significant visual responses at $\sim 20\%$ of the recording sites, whereas MU recordings yielded robust visual responses at nearly all sites (Table 2).

Second, a small percentage of LFP sites, although tuned for speed or direction, yielded responses that were predominantly inhibitory, although the MU activity yielded robust excitation (Fig. 8, Table 2). The MU tuning curve in Figure 8*A* (bottom), for example, exhibits excitatory responses at all speeds tested, whereas the LFP tuning curve (Fig. 8*A*, top) exhibits weak inhibition at most speeds with little or no excitation. Similar differences are evident in the direction tuning curves (Fig. 8*B*). Despite the gross difference in inhibition versus excitation, the preferred direction and speed remained similar for LFP and MU. Nevertheless, we excluded eight tuning curves of this nature [seven speed and one direction (Table 2)] from the population comparison in Figure 4 because our formula for tuning width generated misleading values for predominantly inhibitory tuning curves.

Third, a signal detection analysis revealed that the MU activity typically provides more precise information about the visual stimulus than does the LFP. Using standard ROC methods, we calculated a neuronal threshold for speed discrimination for each

MU and LFP speed tuning curve (for details, see Liu and Newsome, 2005). In essence, the analysis determines the difference in stimulus speed that would support 75% correct performance by an ideal observer who must discriminate between two nearby speeds based on the recorded electrophysiological responses. For this analysis, we chose the best (lowest) discrimination threshold for each tuning curve; this threshold usually corresponded to the point of steepest slope on the tuning curve.

For the MU data, on average, a $92 \pm 5\%$ (mean \pm SEM) difference between the two speeds was necessary to support threshold performance (75% correct). (We defined percentage difference as the absolute difference divided by the faster speed.) In contrast, for LFP activity, a $145 \pm 16\%$ (mean \pm SEM) speed difference was necessary to support threshold performance. When we excluded signals below 40 Hz from the LFP, threshold speed differences fell to $122 \pm 12\%$ (mean \pm SEM). Thus, MU activity encodes the sensory stimulus more precisely than does the conventional LFP, but LFP precision improves for frequencies above 40 Hz.

The superior sensitivity of the MU signal was attributable to the fact that MU tuning curves generally had steeper slopes than the LFP tuning curves, which in turn reflects the fact that the maximum responses of the MU signal were substantially larger relative to the spontaneous activity (see above). The trial-to-trial variance of the LFP responses was actually smaller than the variance of the MU responses, which could in principle lead to lower neural thresholds (variance-to-mean ratio, mean \pm SD, 0.22 ± 0.37 for LFP and 1.23 ± 1.31 for the MU). However, the greater reliability of the signal was not sufficient to overcome the weaker visual responses of the LFP signal.

Choice probability: LFP signals above 40 Hz are correlated with perceptual decisions

CP is a metric that captures trial-to-trial relationships between variable neural responses and variable psychophysical choices for repeated presentations of identical stimuli (see Materials and Methods). A significant CP reflects an unusually close relationship between neural firing and behavior, strengthening the case that the neuron(s) under study contributes to perceptual judgments (Britten et al., 1996; Dodd et al., 2001; Cook and Maunsell, 2002; Uka and DeAngelis, 2004; Barberini et al., 2005; Liu and Newsome, 2005; Purushothaman and Bradley, 2005).

In a previous study, we found that both SU and MU activity in MT exhibited significant CP for perceptual judgments of speed in the discrimination task used in the present study (Liu and Newsome, 2005). We therefore inquired whether the LFP signals also yield significant CP and whether CP values depend on the frequency composition of the LFP signal.

Figure 9*A* shows a scatter plot of CP values calculated for LFP and MU signals at 52 sites in which both signals were recorded as the monkey performed the speed discrimination task. Recall that a CP of 0.5 is consistent with the null hypothesis of no trial-to-trial correlation between firing rates and behavioral judgments, given a constant input stimulus. In contrast, CP values significantly different from 0.5 indicate a nonrandom relationship between neural response and behavioral choice. If a significant CP value is >0.5 , the relationship between neural response and behavioral choice is in the intuitive direction: neurons tuned for high speeds respond more strongly when the monkey judges the stimulus in the RF to move faster than the stimulus outside the RF. CP values <0.5 reflect the counterintuitive result (for a detailed explanation, see Liu and Newsome, 2005).

Visual inspection of Figure 9*A* reveals that the CP of most MU

sites was >0.5 (ordinate), and statistical analysis shows that the effect was significant at the population level (average MU CP of 0.521; t test for difference of the mean from 0.5, $p < 0.002$). In contrast, the standard LFP signal (abscissa) did not exhibit a significant CP effect (mean CP of 0.498; t test, $p = 0.78$). Given our results regarding speed and direction tuning of the LFP, we performed the same CP calculation again, arbitrarily choosing 40 Hz as the cutoff frequency. When frequencies below 40 Hz were excluded from the LFP, the mean CP indeed became significantly greater than chance (mean LFP CP of 0.533; t test, $p < 0.004$) (Fig. 9B). Moreover, such CP values were correlated with the CP values calculated from MU on an experiment-by-experiment basis ($r = 0.45$; $p < 0.001$) (Fig. 9B). CP values calculated from narrow frequency bands (20 Hz wide) became significantly correlated with perceptual choices only when components below 60 Hz were excluded (Fig. 9C).

Somewhat surprisingly, power in the lowest frequency bands (<30 Hz) was anticorrelated with behavioral choices, resulting in CP values significantly <0.5 (Fig. 9C). The magnitude of the anticorrelation at low frequencies (CP of ~ 0.48) was essentially the same as that of the positive correlation at higher frequencies (CP of ~ 0.52). At first glance, this appears consistent with previous reports from electrophysiological and magnetoencephalography studies that visually evoked activity in the alpha and gamma bands is anticorrelated (Fries et al., 2001; Hoogenboom et al., 2006). This was not the case, however, in our data. After equalizing the average LFP power of each stimulus condition (i.e., each speed within the RF aperture), we in fact observed a positive correlation between power in the 0–20 and 60–80 Hz bands (average of 52 recording sites; $r = 0.28$; SEM of 0.03).

MT receives synaptic inputs, of course, from many neural structures, including feedback from higher cortical areas and input from subcortical structures such as the pulvinar nucleus (Maunsell and van Essen, 1983; Ungerleider and Desimone, 1986; Adams et al., 2000). Trial-to-trial variability in LFP power could reflect variability in any of these inputs in addition to variability imposed by feedforward visual inputs. To eliminate all variability in total LFP power across trials, we normalized the power spectrum of each LFP trace such that the total power summed across frequency bands equaled unity. After this normalization for total power on a trial-by-trial basis, we indeed observed an anticorrelation between relative power in the 0–20 and 60–80 Hz bands (mean correlation coefficient of -0.39 ; $p < 10^{-4}$, t test after Fisher's z' transformation). This systematic anticorrelation was not a trivial arithmetic result of normalizing for total power on each trial. For example, the correlation coefficient between 60–80 and 120–140 Hz bands was 0.29 ($p < 10^{-4}$, t test

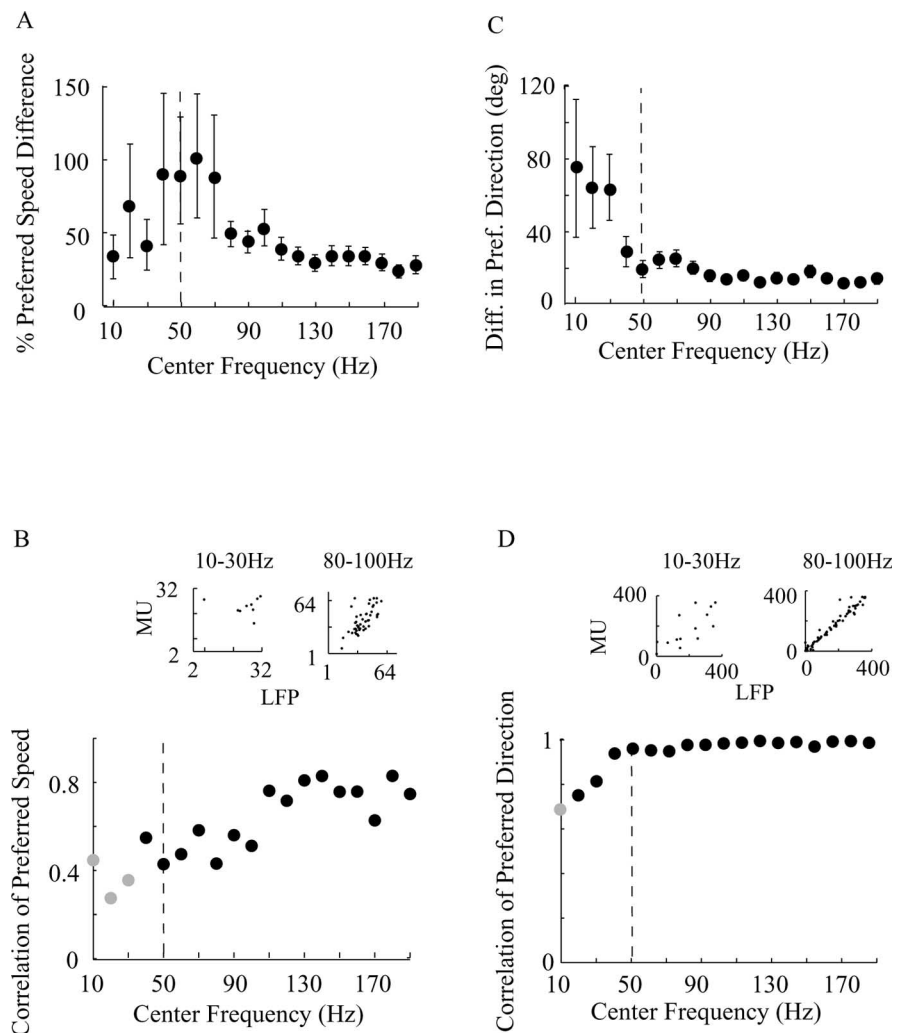


Figure 7. Comparison of tuning parameters derived from MU data and from narrow spectral bands (20 Hz) within the LFP. Adjacent bands were 10 Hz apart. The x -axis indicates the center of each frequency band. **A**, Percentage difference between the preferred speeds derived from LFP and from MU activity, calculated as the absolute difference between preferred speed of LFP and preferred speed of MU, divided by the preferred speed of MU. Error bars indicate the SEM. **B**, Correlation coefficients of LFP preferred speeds and MU preferred speeds. The gray data points were not significantly different from 0 ($p > 0.05$). The insets show scatter plots of the MU preferred speed against LFP preferred speed, for one low-frequency and one high-frequency band. **C**, Mean absolute difference between the preferred directions derived from LFP and from MU data, with SEs. **D**, Correlation coefficients of LFP preferred directions and MU preferred directions. The gray data points were not significantly different from 0 ($p > 0.05$). The insets show scatter plots of the MU preferred directions against LFP preferred direction, for one low-frequency and one high-frequency band.

after Fisher's z' transformation) after the normalization. Rather, the anticorrelation appears to reflect genuine trial-to-trial variation in the temporal structure of the LFP, with lower frequencies having a relative advantage on some trials and higher frequencies on others. We observed this same trial-to-trial anticorrelation between 0–20 and 60–80 Hz LFP power (after normalization) in our speed tuning data obtained while the monkey simply maintained fixation (mean correlation coefficient of -0.31 ; $p < 10^{-4}$, t test after Fisher's z' transformation). Thus, the basic anticorrelation effect is not likely to result from active perceptual discrimination by the monkey.

Finally, we performed the CP analysis on the spectral subbands of the LFP after the trial-by-trial normalization for total power described above; Figure 9D shows the results. The data differ little from the CP values computed before trial-by-trial normalization (Fig. 9C). (Note that a trial-by-trial normalization

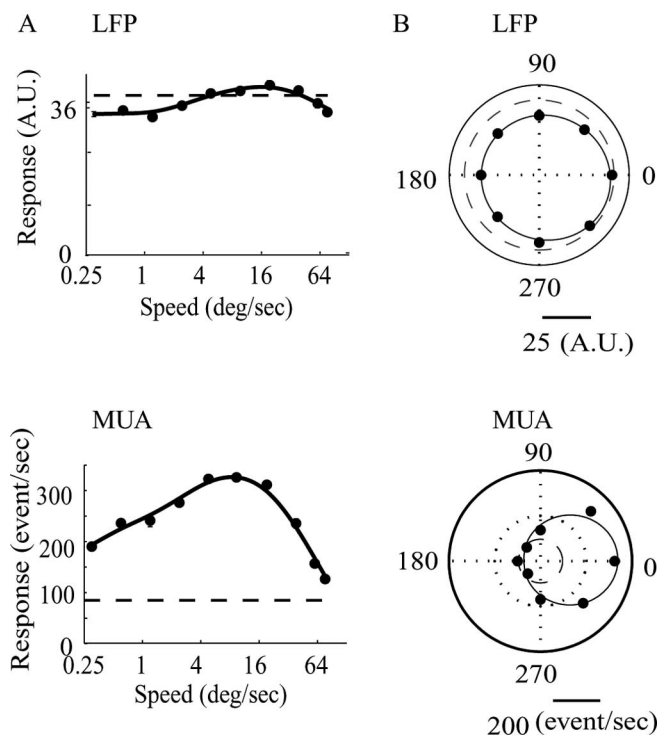


Figure 8. *A*, A speed tuning site in which the LFP was inhibited at nonpreferred speeds. The MU tuning curve has the same shape as LFP, but there is no inhibition at any speed. *B*, The LFP and MU direction tuning curves recorded at the same site. The two curves are similar in shape, but the LFP curve is inhibitory at all directions. The format of *A* and *B* are the same as in Figure 3, in which the dashed lines indicate spontaneous activity. A.U., Arbitrary units; MUA, MU activity.

of total spike count in MU or SU data would, by definition, eliminate the CP effect because every trial would be assigned an identical “firing rate.”) The data in Figure 9*D* imply that the monkey is more likely to decide in favor of the preferred speed at the recording site on trials in which gamma-band power is boosted at the expense of alpha-band power.

Discussion

We compared the properties of MU and LFP signals recorded simultaneously from visual area MT to determine how accurately the LFP reflects the well known columnar (or clustered) architecture of MT and the well documented relationship between MT neural activity and perceptual judgments. Our primary results are that LFP signals at and above the gamma band are well tuned for motion direction and speed and that trial-to-trial fluctuations in the LFP power at and above the gamma band are correlated with perceptual judgments of speed near psychophysical threshold. In all of these respects, the LFP is similar to MU activity recorded simultaneously, demonstrating that the LFP signal above 40 Hz reflects neural activity that is local on a spatial scale equivalent to (or smaller than) that of cortical columns. Our observation of strong tuning for LFP frequencies above 40 Hz is consistent with several recent studies showing that the LFP above 40 Hz seems to carry local information that is difficult to detect at lower frequencies (Siegel and Konig, 2003; Henrie and Shapley, 2005; Niessing et al., 2005).

Exactly why speed and direction tuning deteriorate at lower frequencies is unclear. One possibility is that the cortex acts as a capacitive filter, permitting low-frequency signals to travel longer distances without attenuation than do higher-frequency

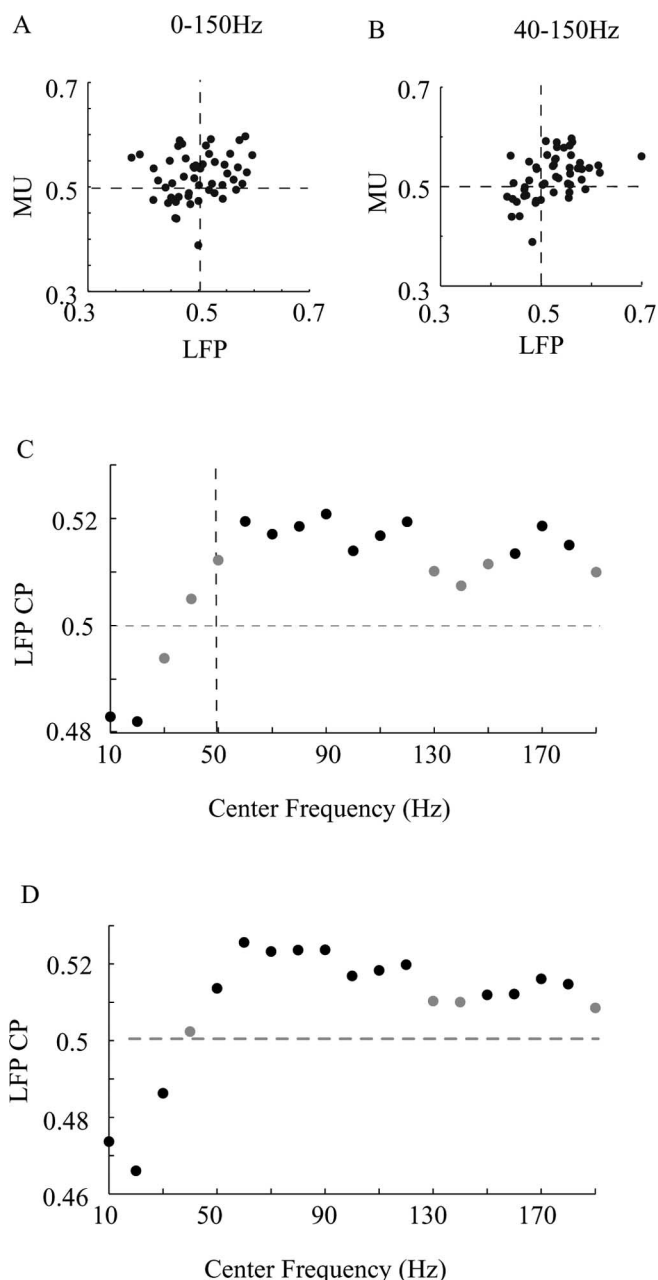


Figure 9. Comparison of CP values calculated from LFP and MU data. *A*, LFP signals (0–150 Hz) did not exhibit significant CP (mean of 0.498). *B*, LFP signals above 40 Hz exhibit significant CP (mean of 0.533), which is also correlated with CP values calculated from MU data. *C*, CP values calculated from narrow frequency sub-bands within the LFP. Each band is 20 Hz wide, and adjacent bands were separated by 10 Hz. x-Axis indicates the center of each frequency band. The black data points are significantly different from 0.5 (*t* test, $p < 0.05$). *D*, CP values calculated from the relative power (the total power of each trial, summed across frequency bands, was normalized to unity) of narrow frequency sub-bands within the LFP. The format is the same as in *C*.

signals (Bédard et al., 2004). Under this hypothesis, speed and direction tuning deteriorate at low frequencies because the signal is spatially “blurred” across multiple cortical columns. Some aspects of our data are consistent with this notion. In particular, it is striking that speed tuning, which is organized on a spatial scale of 300–600 μm (Liu and Newsome, 2003), deteriorates at higher frequencies than does direction tuning, which is organized on a spatial scale of up to 2 mm in columns perpendicular to the cortical surface (Albright et al., 1984; DeAngelis and Newsome,

1999; Liu and Newsome, 2003). A recent study that compared MU with LFP tuning in inferotemporal cortex is also consistent with the “capacitive filtering” interpretation of our data (Kreiman et al., 2006). These investigators built a simple model that combined successive MU recordings along a penetration to identify the spatial range of signals that best accounted for tuning in the LFP. They concluded that their LFP measurements, which were dominated by signals below 40 Hz, were best explained by a weighted average of MU signals within 3 mm of the LFP recording site. This range of spatial spread in the low-frequency range would certainly account for the loss of direction and speed tuning in our LFP recordings.

Conversely, direct experimental measurements suggest that the cortex does not act as a capacitive filter and that the impedance spectrum of the cortex is in fact nearly flat. This observation was first made in a study of rabbit cortex (Ranck, 1963) and has recently been confirmed through detailed measurements in monkey cortex (N. Logothetis, personal communication). Loss of stimulus tuning at low frequencies, although more difficult to explain from this point of view, might be related to slow, global, neuromodulatory effects in the cortex, to differential effects of desynchronization on experimental measurements of low- versus high-frequency LFP signals, or to as yet unidentified sources of noise in the lowest frequency ranges. Future studies will be necessary to address this problem.

Comparison with previous studies

Several recent studies have demonstrated close relationships between gamma-band LFP power and visual stimulus properties, including orientation selectivity (Frien and Eckhorn, 2000), spatial and temporal frequency selectivity (Kayser and König, 2004), and contrast–response functions with shapes similar to those of SU recorded simultaneously (Henrie and Shapley, 2005). Gamma-band power can also reflect local signal processing that is not strictly related to a sensory stimulus. Pesaran et al. (2002) and colleagues, for example, show that gamma-band power recorded from macaque parietal cortex exhibits spatial tuning during a memory-guided saccade task. What our study critically adds is a careful comparison of LFP tuning with that of MU signals recorded simultaneously from a neural structure with a well characterized spatial architecture.

The LFP and the blood oxygenation level-dependent response

The spectral frequency dependence of LFP tuning has interesting implications for understanding the blood oxygenation level-dependent (BOLD) response, the metric underlying functional magnetic resonance imaging. Under many experimental conditions, the BOLD response is well correlated with both unit activity (Rees et al., 2000; Mukamel et al., 2005) and with the LFP (Logothetis et al., 2001). Under conditions in which the LFP can be dissociated from unit activity, however, the BOLD response appears much better correlated with the LFP (Mathiesen et al., 1998, 2000). In light of the current results, it would be interesting to know whether the correlation between the BOLD signal and the LFP is itself frequency dependent. Is the correlation particularly tight within a specific frequency band of the LFP, or does the correlation draw from all frequencies? Such data may permit interesting inferences about localization of the BOLD signal itself.

Two recent studies have reported that variations in the hemodynamic response in cats is more tightly correlated with synchronized gamma-band activity than with activity in any other band of the LFP or with spike rate, at least under certain stimulus

conditions (Kayser et al., 2004; Niessing et al., 2005). If so, the correspondence between perceptual choices and increased gamma power that we demonstrated here (CP) (Fig. 9C,D) might be detectable in the BOLD signal as well.

Spectral contamination from spikes?

A potentially trivial explanation for the high correlation we observed for tuning of LFP and MU activity is that our LFP signal is dominated by low-frequency components of individual spikes. Although LFP signals are commonly thought to reflect summed synaptic currents (for review, see Mitzdorf, 1985), it is inevitable that some low-frequency components of individual action potentials will contribute to the LFP, particularly in the higher-frequency range of the LFP.

For several reasons, however, we do not believe that the tuning of our LFP signals arises predominantly from low-frequency spectral components of action potentials. First, speed and direction tuning become weaker for the highest frequency components of our LFP measurements (Figs. 5, 6); which should not be true if tuning derives primarily from action potentials (Henrie and Shapley, 2005). Second, direction tuning remains strong in the 40–80 Hz band of the LFP, whereas speed tuning deteriorates markedly in the same range (Fig. 7). This difference is difficult to explain by invoking spectral contamination from spikes recorded simultaneously with the LFP but follows naturally from the view that low-frequency signals from synaptic currents propagate through the cortex in a frequency-dependent manner (see above). Finally, the MU and LFP recordings differed from each other substantially in certain respects, the most notable being the occasional sites at which inhibitory LFP responses and excitatory MU activity were recorded simultaneously. Although spikes almost certainly contribute partially to our LFP signals, it is unlikely that the primary results of our study are attributable to such contamination.

The LFP and choice probability

An important result of our study is that the LFP, used carefully, can reveal trial-to-trial associations between perceptual judgments and the underlying neural activity, which suggests a close functional link between the local population of neurons and the specific behavior under study (for review, see Parker et al., 2002). CP has been demonstrated previously at the SU level for perceptual judgments of motion direction (Britten et al., 1996; Barberini et al., 2005; Purushothaman and Bradley, 2005), motion speed (Liu and Newsome, 2005), coarse binocular disparity (Uka and DeAngelis, 2004), structure-from-motion (Bradley et al., 1998; Dodd et al., 2001), and for detection of coherent motion onset (Cook and Maunsell, 2002). To our knowledge, the current data provide the first demonstration of a CP effect for LFP signals, but the effect was detectable only for frequencies above 40 Hz. Our result complements those of other laboratories that have reported a relationship between the temporal structure of local neural activity and behavior (Fries et al., 2001; Taylor et al., 2005; Womelsdorf et al., 2006).

We were not surprised by the existence of CP effects in the LFP. At the SU level, the CP is thought to arise from variation in correlated activity (presumably arising from common synaptic inputs) within the pool of sensory neurons that contribute to a given perceptual decision (Britten et al., 1992; Zohary et al., 1994; Shadlen et al., 1996). If this is so, one might even have expected the CP to be larger in the LFP than in SU data because activity variation unique to individual cells should be averaged out in the LFP. Our data indicate that future inves-

tigations can use the LFP, filtered to a restricted frequency range, to monitor relationships between local fluctuations in neural activity and perceptual judgments. This capability may prove particularly useful in studies in which SU isolation is difficult to achieve, such as human electrophysiological recordings or chronic electrode arrays in which recording efficacy deteriorates with the passage of time.

Surprisingly, we observed an anticorrelation between low-frequency LFP power (<30 Hz) and behavioral choices (CP <0.5). This effect results from a trial-to-trial anticorrelation between low-frequency and gamma-band LFP power, but this anticorrelation is only observed if the power spectra of the LFP are first normalized for fluctuations in total power from trial to trial (see Results). In other words, behavioral choices are linked to a shift in relative power between low-frequency bands and the gamma band that occurs despite much larger trial-to-trial modulations of LFP power distributed broadly over the entire frequency range of the LFP. The underlying trial-to-trial anticorrelation in relative power between low- and high-frequency bands of the LFP is not dependent on behavioral choice per se; the basic phenomenon exists also in our speed tuning data obtained while the monkey simply maintained fixation. Rather, trial-to-trial shifts in relative power within the LFP appear to reflect natural statistical variation in the local neural response to repeated presentations of a visual stimulus, not dissimilar from the statistical variations in spike count observed in single or multi-neuron recordings. Our data show that perceptual choices (CP) are weakly linked to both phenomena: variations in spike count as well as shifts in relative power within the LFP. Whether these two phenomena result from the same or different underlying cellular mechanisms and whether either or both are causally related to perceptual choices are important issues for future study.

References

- Adams MM, Hof PR, Gattass R, Webster MJ, Ungerleider LG (2000) Visual cortical projections and chemoarchitecture of macaque monkey pulvinar. *J Comp Neurol* 419:377–393.
- Albright TD, Desimone R, Gross CG (1984) Columnar organization of directionally selective cells in visual area MT of the macaque. *J Neurophysiol* 51:16–31.
- Barberini CL, Cohen MR, Wandell BA, Newsome WT (2005) Cone signal interactions in direction-selective neurons in the middle temporal visual area (MT). *J Vis* 5:603–621.
- Bédard C, Kröger H, Destexhe A (2004) Modeling extracellular field potentials and the frequency-filtering properties of extracellular space. *Biophysical J* 86:1829–1842.
- Bradley DC, Chang GC, Andersen RA (1998) Encoding of three-dimensional structure-from-motion by primate area MT neurons. *Nature* 392:714–717.
- Britten K, Shadlen M, Newsome W, Movshon J (1992) The analysis of visual motion: a comparison of neuronal and psychophysical performance. *J Neurosci* 12:4745–4765.
- Britten KH, Newsome WT, Shadlen MN, Celebrini S, Movshon JA (1996) A relationship between behavioral choice and the visual responses of neurons in macaque MT. *Vis Neurosci* 13:87–100.
- Cook EP, Maunsell JH (2002) Dynamics of neuronal responses in macaque MT and VIP during motion detection. *Nat Neurosci* 5:985–994.
- DeAngelis GC, Newsome WT (1999) Organization of disparity-selective neurons in macaque area MT. *J Neurosci* 19:1398–1415.
- Dodd JV, Krug K, Cumming BG, Parker AJ (2001) Perceptually bistable three-dimensional figures evoke high choice probabilities in cortical area MT. *J Neurosci* 21:4809–4821.
- Frien A, Eckhorn R (2000) Functional coupling shows stronger stimulus dependency for fast oscillations than for low-frequency components in striate cortex of awake monkey. *Eur J Neurosci* 12:1466–1478.
- Frien A, Eckhorn R, Bauer R, Woelbern T, Gabriel A (2000) Fast oscillations display sharper orientation tuning than slower components of the same recordings in striate cortex of the awake monkey. *Eur J Neurosci* 12:1453–1465.
- Fries P, Reynolds JH, Rorie AE, Desimone R (2001) Modulation of oscillatory neuronal synchronization by selective visual attention. *Science* 291:1905–1906.
- Fries P, Schroder JH, Roelfsema PR, Singer W, Engel AK (2002) Oscillatory neuronal synchronization in primary visual cortex as a correlate of stimulus selection. *J Neurosci* 22:3739–3754.
- Gail A, Brinksmeier HJ, Eckhorn R (2004) Perception-related modulations of local field potential power and coherence in primary visual cortex of awake monkey during binocular rivalry. *Cereb Cortex* 14:300–313.
- Gray CM, Singer W (1989) Stimulus-specific neuronal oscillations in orientation columns of cat visual cortex. *Proc Natl Acad Sci USA* 86:1698–1702.
- Green DM, Swets JA (1966) Signal detection theory and psychophysics. New York: Wiley.
- Henrie JA, Shapley R (2005) LFP power spectra in V1 cortex: the graded effect of stimulus contrast. *J Neurophysiol* 94:479–490.
- Hoogenboom N, Schoffelen JM, Oostenveld R, Parkes LM, Fries P (2006) Localizing human visual gamma-band activity in frequency, time and space. *NeuroImage* 29:764–773.
- Kayser C, Konig P (2004) Stimulus locking and feature selectivity prevail in complementary frequency ranges of V1 local field potentials. *Eur J Neurosci* 19:485–489.
- Kayser C, Kim M, Uğurbil K, Kim DS, Konig P (2004) A comparison of hemodynamic and neural responses in cat visual cortex using complex stimuli. *Cereb Cortex* 14:881–891.
- Kreiman G, Hung CP, Kraskov A, Quiroga RQ, Poggio T, Dicarlo JJ (2006) Object selectivity of local field potentials and spikes in the macaque inferior temporal cortex. *Neuron* 49:433–445.
- Krug K (2004) A common neuronal code for perceptual processes in visual cortex? Comparing choice and attentional correlates in V5/MT. *Philos Trans R Soc Lond B Biol Sci* 359:929–941.
- Kruse W, Eckhorn R (1996) Inhibition of sustained gamma oscillations (35–80 Hz) by fast transient responses in cat visual cortex. *Proc Natl Acad Sci USA* 93:6112–6117.
- Liu J, Newsome WT (2003) Functional organization of speed tuned neurons in visual area MT. *J Neurophysiol* 89:246–256.
- Liu J, Newsome WT (2005) Correlation between speed perception and neural activity in the middle temporal visual area. *J Neurosci* 25:711–722.
- Logothetis NK (2003) The underpinnings of the BOLD functional magnetic resonance imaging signal. *J Neurosci* 23:3963–3971.
- Logothetis NK, Pauls J, Augath M, Trinath T, Oeltermann A (2001) Neurophysiological investigation of the basis of the fMRI signal. *Nature* 412:128–130.
- Lopes da Silva F (2004) Functional localization of brain sources using EEG and/or MEG data: volume conductor and source models. *Magn Reson Imaging* 22:1533–1538.
- Mardia KV (1972) Statistics of directional data. London: Academy.
- Mathiesen C, Caesar K, Akgoren N, Lauritzen M (1998) Modification of activity-dependent increases of cerebral blood flow by excitatory synaptic activity and spikes in rat cerebellar cortex. *J Physiol (Lond)* 512:555–566.
- Mathiesen C, Caesar K, Lauritzen M (2000) Temporal coupling between neuronal activity and blood flow in rat cerebellar cortex as indicated by field potential analysis. *J Physiol (Lond)* 523:235–246.
- Maunsell JHR, van Essen DC (1983) Functional properties of neurons in middle temporal visual area of the macaque monkey. I. Selectivity for stimulus direction, speed and orientation. *J Neurophysiol* 49:1127–1147.
- Mitzdorf U (1985) Current source-density method and application in cat cerebral cortex: investigation of evoked potentials and EEG phenomena. *Physiol Rev* 65:37–100.
- Mitzdorf U (1987) Properties of the evoked potential generators: current source-density analysis of visually evoked potentials in the cat visual cortex. *Int J Neurosci* 33:33–59.
- Mukamel R, Gelbard H, Arieli A, Hasson U, Fried I, Malach R (2005) Coupling between neuronal firing, field potentials, and FMRI in human auditory cortex. *Science* 309:951–954.
- Niessing J, Ebisch B, Schmidt KE, Niessing M, Singer W, Galuske RA (2005) Hemodynamic signals correlate tightly with synchronized gamma oscillations. *Science* 309:948–951.
- Parker AJ, Krug K, Cumming BG (2002) Neuronal activity and its links with

- the perception of multi-stable figures. *Philos Trans R Soc Lond B Biol Sci* 357:1053–1062.
- Pesaran B, Pezaris JS, Sahani M, Mitra PP, Andersen RA (2002) Temporal structure in neuronal activity during working memory in macaque parietal cortex. *Nat Neurosci* 5:805–811.
- Purushothaman G, Bradley DC (2005) Neural population code for fine perceptual decisions in area MT. *Nat Neurosci* 8:99–106.
- Ranck JB (1963) Specific impedance of rabbit cerebral cortex. *Exp Neurol* 7:144–152.
- Rees G, Friston K, Koch C (2000) A direct quantitative relationship between the functional properties of human and macaque V5. *Nat Neurosci* 3:716–723.
- Rickert J, Oliveira SC, Vaadia E, Aertsen A, Rotter S, Mehring C (2005) Encoding of movement direction in different frequency ranges of motor cortical local field potentials. *J Neurosci* 25:8815–8824.
- Scherberger H, Jarvis MR, Andersen RA (2005) Cortical local field potential encodes movement intentions in the posterior parietal cortex. *Neuron* 46:347–354.
- Shadlen MN, Britten KH, Newsome WT, Movshon JA (1996) A computational analysis of the relationship between neuronal and behavioral responses to visual motion. *J Neurosci* 16:1486–1510.
- Shiklin EV, Plis AI (1995) *Handbook on splines for the user*. Boca Raton, FL: CRC.
- Siegel M, Konig P (2003) A functional gamma-band defined by stimulus-dependent synchronization in area 18 of awake behaving cats. *J Neurosci* 23:4251–4260.
- Taylor K, Mandon S, Freiwald WA, Kreiter AK (2005) Coherent oscillatory activity in monkey area v4 predicts successful allocation of attention. *Cereb Cortex* 15:1424–1437.
- Uka T, DeAngelis GC (2004) Contribution of area MT to stereoscopic depth perception; choice-related response modulations reflect task strategy. *Neuron* 42:297–310.
- Ungerleider LG, Desimone R (1986) Cortical connections of visual area MT in the macaque. *J Comp Neurol* 248:190–222.
- van Essen DC, Maunsell JHR, Bixby JL (1981) The middle temporal visual area in the macaque: myeloarchitecture, connections, functional properties and topographic organization. *J Comp Neurol* 199:293–326.
- Widrow B, Glover JR, McCool JM, Kaunitz J, Williams CS, Haearn RH, Zeidler JR, Dong E, Goodlin RC (1975) Adaptive noise cancelling: principles and applications. *Proc IEEE* 63:1692–1716.
- Womelsdorf T, Fries P, Mitra PP, Desimone R (2006) Gamma-band synchronization in visual cortex predicts speed of change detection. *Nature* 439:733–736.
- Zohary E, Shadlen MN, Newsome WT (1994) Correlated neuronal discharge rate and its implications for psychophysical performance. *Nature* 370:140–143.